NONLINEAR BEHAVIOUR OF CAPILLARY-GRAVITY WAVES NEAR THE INFLECTION POINT OF THE DISPERSION CURVE

Oikawa, Masayuki
Research Institute for Applied Mechanics, Kyushu University : Professor

https://doi.org/10.5109/6783296

出版情報：Reports of Research Institute for Applied Mechanics. 38 (108), pp.61-81, 1991-09. 九州大学応用力学研究所

Note

Reports of Research Institute for Applied Mechanics
Vol. XXXVIII, No. 108, 1991

NONLINEAR BEHAVIOUR OF CAPILLARY-GRAVITY WAVES NEAR THE INFLECTION POINT OF THE DISPERSION CURVE

By Masayuki OIKAWA*

A modified nonlinear Schrödinger equation (MNLS) is derived to describe a finite-amplitude capillary-gravity wavepacket near the inflection point of the dispersion curve. Modulational stability of a uniform wavetrain for an infinitesimal disturbance is examined on the basis of the MNLS. Nonlinear evolution of a periodic disturbance is computed by using a pseudospectral method. It is found that nonlinear evolution of a periodic disturbance based on MNLS is qualitatively different from that based on the nonlinear Schrödinger equation. We also mention the double-hump solitary wave solutions found by Akylas and Kung.

Key words: Capillary-gravity wave, Modified nonlinear Schrödinger equation, Modulational instability, Double-hump solitary wave

1. Introduction

Weak nonlinear modulation of capillary-gravity water waves is described by the nonlinear Schrödinger equation (NLS)[1]. However, the NLS breaks down near the inflection point of the dispersion curve. We derive in § 2 a modified nonlinear Schrödinger equation (MNLS) which takes the place of the NLS near the point. Recently, the MNLS was investigated by Akylas and Kung[2]. They searched permanent wave envelope solutions of the MNLS to find double-hump solitary wave solutions. In this note we mainly investigate the time evolution of the solutions of the MNLS. For this purpose we solve numerically the MNLS

* Professor, Research Institute for Applied Mechanics, Kyushu University.

by using a pseudospectral method.

In § 3, we examine the stability characteristics of the uniform wave solution of the MNLS to modulation perturbations. The MNLS possesses a high wavenumber cutoff in the instability characteristics as the NLS does. Yuen and Ferguson[3] investigated the long time evolution of the modulationally unstable disturbances for the uniform wave solutions of the NLS under the periodic boundary condition. According to their numerical computation, the number of modes which actively participate in the energy sharing process associated with the instability is governed by the number of harmonics of the initial disturbance which lie within the unstable region. Then, Yuen and Ferguson proposed that with periodic boundary conditions, a near-uniform solution undergoing long-wave instability would not thermalize if there is a high-wavenumber cutoff in the instability characteristics. In § 4, we report the numerical results of the time evolutions of the unstable periodic disturbances for both the MNLS and for the NLS. It is found that the time evolution of the disturbance in the MNLS is qualitatively different from that in the NLS. It seems that the proposal of Yuen and Ferguson is not applicable to the MNLS.

In § 5, the numerical solution of the MNLS for a localized initial wave packet is presented. We mention the double-hump solitary wave solutions to the MNLS in § 6.

2. Modified Nonlinear Schrödinger Equation

The capillary-gravity waves on deep water have the dispersion relation

$$\omega^2 = gk + \frac{T}{\rho}k^3. \tag{1}$$

Here k is the wavenumber, ω is the angular frequency, g is the gravitational acceleration, T is the surface tension and ρ is the density. The weakly nonlinear modulations of them are usually described by the NLS. However, the NLS breaks down near the inflection point ($d^2\omega/dk^2=0$) of the dispersion curve, that is, near the point

$$k = k_c \equiv \left(\alpha\frac{\rho g}{T}\right)^{1/2}, \quad \alpha = \frac{2\sqrt{3}-3}{3} = 0.1547\cdots. \tag{2}$$

In order to examine nonlinear behaviour of the capillary-gravity wave in the vicinity of $k=k_c$, we normalize the variables as follows:

$$\left.\begin{aligned} &k_c x' = x, \quad k_c y' = y, \quad \sqrt{gk_c}\,t' = t, \\ &\frac{\eta'}{a} = \eta, \quad \varphi'\Big/\left(\frac{\sqrt{gk_c}}{k_c}a\right) = \varphi, \end{aligned}\right\} \tag{3}$$

where x and y are the horizontal and vertical coordinates, respectively, t is the time, η is the free surface displacement, φ is the velocity potential and a is the characteristic amplitude of the wave. The variables with the prime are dimensional ones. Then, the governing system of equations are

$$\varphi_{xx}+\varphi_{yy}=0, \quad -\infty<y<\varepsilon\eta, \tag{4}$$

$$\varphi\to 0 \quad \text{as} \quad y\to-\infty, \tag{5}$$

$$\eta_t+\varepsilon\varphi_x\eta_x=\varphi_y \quad \text{at} \quad y=\varepsilon\eta, \tag{6}$$

$$\varphi_t+\frac{1}{2}\varepsilon(\varphi_x^2+\varphi_y^2)+\eta=\alpha(\eta_x/\sqrt{1+\varepsilon^2\eta_x^2})_x, \quad \text{at} \quad y=\varepsilon\eta, \tag{7}$$

where $\varepsilon\equiv ak_c$ is the wave steepness. We assume the following expansions:

$$\begin{aligned}\varphi=&\ \varphi^{(1)}(X,\ T,\ y)e^{i\theta}+\text{c. c.}\\ &+\varepsilon[\varphi^{(2)}(X,\ T,\ y)e^{2i\theta}+\text{c. c.}+\varphi^{(0)}(X,\ T,\ y)]+\cdots,\end{aligned} \tag{8}$$

$$\begin{aligned}\eta=&\ \eta^{(1)}(X,\ T)e^{i\theta}+\text{c. c.}\\ &+\varepsilon[\eta^{(2)}(X,\ T)e^{2i\theta}+\text{c. c.}+\eta^{(0)}(X,\ T)]+\cdots.\end{aligned} \tag{9}$$

Here

$$\theta=kx-\omega t, \quad \omega=(k+\alpha k^3)^{1/2} \tag{10}$$

and

$$X=\varepsilon^{2/3}(x-c_g t), \quad T=\varepsilon^2 t \quad (c_g\equiv\frac{d\omega}{dk}). \tag{11}$$

The leading terms of $\varphi^{(1)}$, $\eta^{(1)}$, $\cdots$ are $O(1)$. Solving eqs.(4) and (5) successively up to $O(\varepsilon^2)$, we obtain

$$\begin{aligned}\varphi^{(1)}=&-\frac{i\omega}{k}B(X,\ T)e^{ky}-\varepsilon^{2/3}\frac{\omega}{k}\frac{\partial B}{\partial X}ye^{ky}\\ &+\varepsilon^{4/3}\frac{i\omega}{2k}\frac{\partial^2 B}{\partial X^2}y^2e^{ky}+\varepsilon^2\frac{\omega}{6k}\frac{\partial^3 B}{\partial X^3}y^3e^{ky}+\cdots.\end{aligned} \tag{12}$$

We also obtain from eq.(6)

$$\begin{aligned}\eta^{(1)}=&\ \frac{i}{\omega}\frac{\partial\varphi^{(1)}}{\partial y}-\varepsilon^{2/3}\frac{c_g}{\omega^2}\frac{\partial^2\varphi^{(1)}}{\partial X\partial y}-\varepsilon^{4/3}\frac{ic_g^2}{\omega^3}\frac{\partial^3\varphi^{(1)}}{\partial X^2\partial y}+\varepsilon^2\Big(\frac{c_g^3}{\omega^4}\frac{\partial^4\varphi^{(1)}}{\partial X^3\partial y}\\ &+\frac{1}{\omega^2}\frac{\partial^2\varphi^{(1)}}{\partial T\partial y}-\frac{2k^2}{\omega^2}\varphi^{(2)}\frac{\partial\varphi^{(1)*}}{\partial y}-\frac{2ik^2}{\omega}\eta^{(2)}\varphi^{(1)*}+\frac{ik^2}{\omega^3}\Big(\frac{\partial\varphi^{(1)}}{\partial y}\Big)\frac{\partial\varphi^{(1)*}}{\partial y}\\ &+\frac{i}{\omega}\eta^{(2)}\frac{\partial^2\varphi^{(1)*}}{\partial y^2}+\frac{1}{\omega^2}\frac{\partial^2\varphi^{(2)}}{\partial y^2}\frac{\partial\varphi^{(1)*}}{\partial y}+\frac{i}{\omega}\eta^{(0)}\frac{\partial^2\varphi^{(1)}}{\partial y^2}\\ &-\frac{i}{2\omega^3}\Big(\frac{\partial\varphi^{(1)}}{\partial y}\Big)^2\frac{\partial^3\varphi^{(1)*}}{\partial y^3}+\frac{i}{\omega^3}\frac{\partial\varphi^{(1)}}{\partial y}\frac{\partial\varphi^{(1)*}}{\partial y}\frac{\partial^3\varphi^{(1)}}{\partial y^3}\Big)+\cdots, \quad \text{at} \quad y=0,\\ =&\ B(X,\ T)+\cdots.\end{aligned} \tag{13}$$

Eliminating $\eta^{(1)}$ from eq. (7) by use of (13) and using eq. (12) and the lowest order approximations

$$\eta^{(2)}=\frac{\omega^2B^2}{1-2\alpha k^2}, \quad \varphi^{(2)}=-\frac{3i\alpha\omega k^2B^2}{1-2\alpha k^2}e^{2ky}, \quad \eta^{(0)}=\varphi^{(0)}=0,$$

we have the solvability condition up to $O(\varepsilon^2)$:

$$
\Big[\omega^2-(k+ak^3)\Big]B-\varepsilon^{2/3}i\Big[2\omega\omega'-(1+3ak^2)\Big]\frac{\partial B}{\partial X}
+\varepsilon^{4/3}(3ak-\omega'^2)\frac{\partial^2 B}{\partial X^2}+\varepsilon^2\Big\{2i\omega\frac{\partial B}{\partial T}-i\Big(\frac{\omega'^3}{\omega}+a-\frac{3ak\omega'}{\omega}\Big)\frac{\partial^3 B}{\partial X^3}
-\frac{k^3(8+ak^2+2a^2k^4)}{2(1-2ak^2)}|B|^2B\Big\}=0, \tag{14}
$$

where $\omega'\equiv d\omega/dk=c_g$. Owing to eq. (10), the first and second terms in eq. (14) vanish, and

$$
\omega''\equiv\frac{d^2\omega}{dk^2}=\frac{3ak-\omega'^2}{\omega}=\frac{3a^2k^4+6ak^2-1}{4\omega^3}, \tag{15}
$$

$$
\omega'''\equiv\frac{d^3\omega}{d\omega^3}=\frac{3}{\omega}\Big(\frac{\omega'^3}{\omega}+a-\frac{3ak\omega'}{\omega}\Big)
=\frac{3}{8\omega^5}(1-ak^2)(1+6ak^2+a^2k^4). \tag{16}
$$

Assuming $\omega''=O(\varepsilon^{2/3})$, we obtain

$$
i\frac{\partial B}{\partial T}+\frac{\omega''}{2\varepsilon^{2/3}}\frac{\partial^2 B}{\partial X^2}-\frac{i}{6}\omega'''\frac{\partial^3 B}{\partial X^3}-\nu|B|^2B=0,
\quad \nu=\frac{k^3(8+ak^2+2a^2k^4)}{4\omega(1-2ak^2)}. \tag{17}
$$

From the definition of a and eq. (15), $\omega''<0$ for $k<1$, $\omega''=0$ for $k=1$ and $\omega''>0$ for $k>1$. Since we consider the neighbourhood of $k=1$, ω''' and ν may be taken to be positive. Then, the transformation

$$
B=\nu^{-1/2}A \tag{18}
$$

gives rise to the MNLS

$$
i\frac{\partial A}{\partial T}-\beta\frac{\partial^2 A}{\partial X^2}-i\gamma\frac{\partial^3 A}{\partial X^3}-|A|^2A=0, \tag{19}
$$

where

$$
\beta=-\frac{\omega''}{2\varepsilon^{2/3}},\quad \gamma=\frac{1}{6}\omega'''. \tag{20}
$$

3. Modulational Instability of the Uniform Wave Solution

The solution to the MNLS (19) describing the uniform nonlinear wavetrain is given by

$$
A_0=a_0\exp(-ia_0^2T+ib_0), \tag{21}
$$

where a_0 is an arbitrary positive constant and b_0 is an arbitrary real constant. In order to examine the modulational stability characteristics of the solution (21), we consider the perturbed solution

$$
A=(a_0+\hat{a}(X,\ T))\exp\{-ia_0^2T+ib_0+i\hat{\theta}(X,\ T)\}. \tag{22}
$$

Introducing the expression (22) into eq. (19), linearizing with respect to $\hat{a}$ and $\hat{\theta}$ and putting

$$(\hat{a},\ \hat{\theta}) \quad \propto \quad e^{i(\kappa X - \Omega T)}, \tag{23}$$

we have

$$\Omega = \gamma \kappa^3 \pm \sqrt{\kappa^2(\beta^2\kappa^2 - 2\beta a_0^2)}. \tag{24}$$

As a result, if $\beta < 0$ (*i.e.* $k > 1$), the solution (21) is stable. On the other hand, if $\beta > 0$ (*i.e.* $k < 1$), (21) is unstable for $0 < \kappa < \kappa_c\ (\equiv \sqrt{2/\beta}\, a_0)$. The stability characteristics do not depend on γ and are the same as in the case of the NLS. Especially, there is the high-wavenumber cutoff κ_c in the instability characteristics.

4. Time Evolution of an Unstable Periodic Disturbance

Yuen and Ferguson[3] investigated numerically the long time evolution of the solution of the NLS with the periodic boundary condition starting from the initial condition

$$A(X,\ 0) = a_0[1 - 0.1\cos(\kappa X)], \quad 0 \le X \le L, \tag{25}$$

where $L = 2\pi/\kappa$. They found that if $0 < n\kappa < \kappa_c$ and $\kappa_c < (n+1)\kappa$, n modes actively participated in the energy sharing process associated with the instability.

In this section we present the numerical results of the time evolution of the solutions of the MNLS (19) for the initial conditions (25). Incidentally, we also present the results of the same problem for the NLS

$$i\frac{\partial A}{\partial T} - \beta\frac{\partial^2 A}{\partial X^2} - |A|^2 A = 0, \tag{26}$$

because we want to compare the solutions of the MNLS with those of the NLS

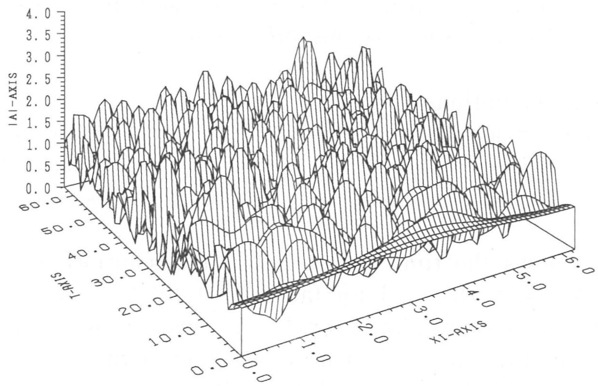

(a)

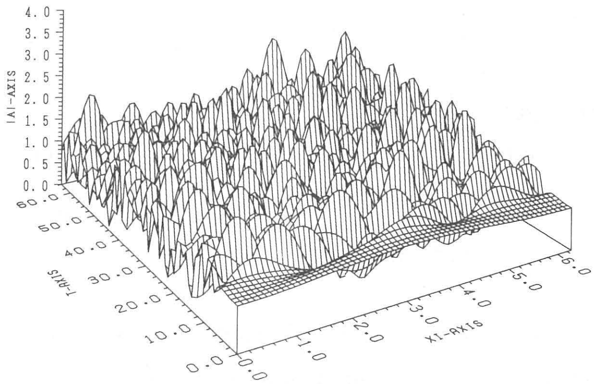

(b)

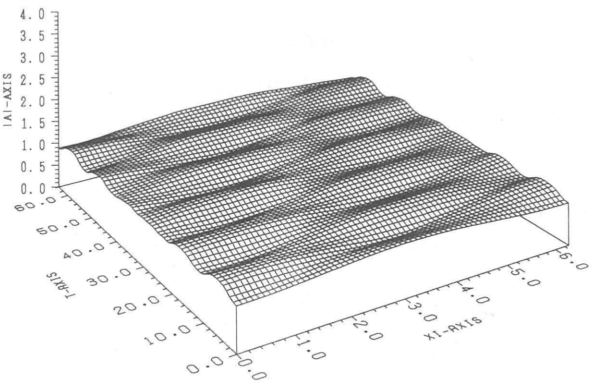

(c)

Fig. 1 The envelope amplitude $|A|$ of the solutions to the MNLS for $A(X, 0)=1-0.1\cos X$. $\varepsilon=0.05$. (a)$k=0.9$, (b)$k=1$, (c)$k=1.1$.

under the same conditions.

A pseudospectral method[4] was employed for the numerical computations. In all the calculations, the conserved quantity $\int|A|^2dX$ of eqs. (19) and (26) was conserved within a sufficient accuracy. Throughout this paper we take $\varepsilon = 0.05$ and $a_0 = 1$.

Figure 1 shows the time evolutions of the solutions to the MNLS (19) starting from (25) with $\varkappa = 1$ for (a) $k = 0.9$, (b) $k = 1$ and (c) $k = 1.1$. The figures in this section are ploted for $\xi = \varkappa X$ instead of X. The behaviours of the solutions in Fig. 1(a) and (c) are consistent with the result of the linear stability analysis. In the case $k = 1$, the uniform state becomes unstable due to nonlinear effect, though it neutrally stable in the linear analysis.

Figure 2 shows the solutions to the MNLS (19) starting from (25) with

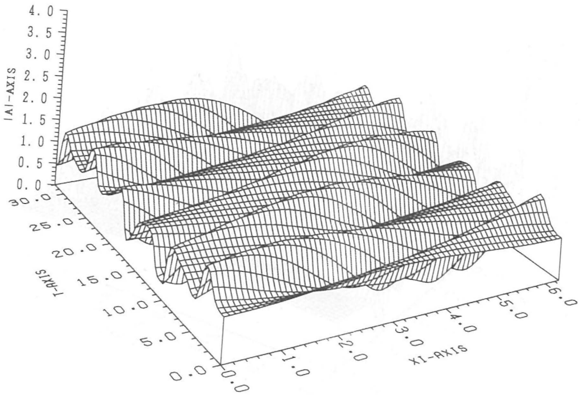

(a)

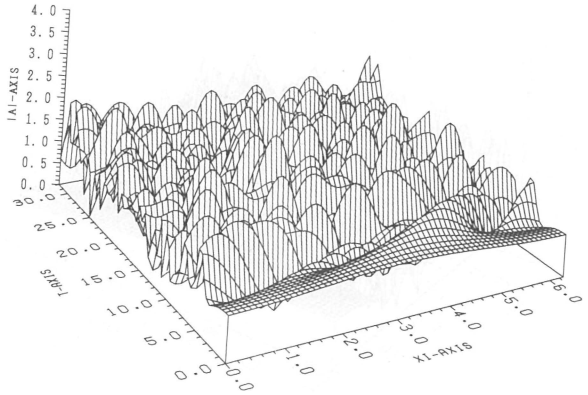

(b)

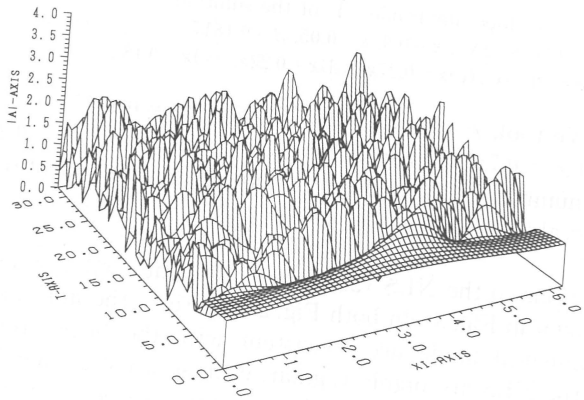

(c)

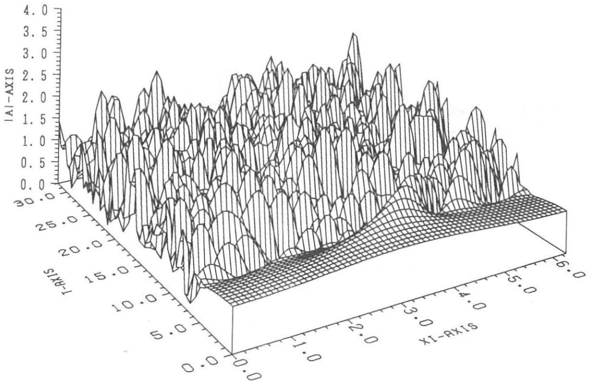

(d)

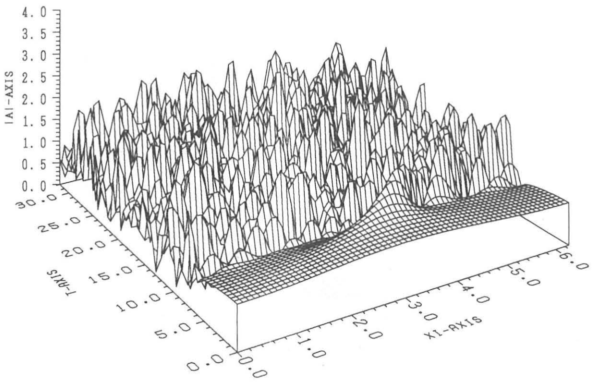

(e)

Fig. 2 The envelope amplitude $|A|$ of the solutions to the MNLS for $A(X, 0) = 1 - 0.1\cos(\varkappa X)$. $\varkappa = 0.9$, $\varepsilon = 0.05$, $\beta = 0.1817 \cdots$, $\gamma = 0.0936 \cdots$. (a)$\varkappa = 0.7\varkappa_c$, (b)$\varkappa = 0.35\varkappa_c$, (c)$\varkappa = 0.27\varkappa_c$, (d)$\varkappa = 0.22\varkappa_c$, (e)$\varkappa = 0.18\varkappa_c$.

different $\varkappa$. We took $k = 0.9$, $\varepsilon = 0.05$ so that $\beta = 0.1817\cdots$. The values of $\varkappa$ chosen are (a) $\varkappa = 0.7\varkappa_c$, (b) $\varkappa = 0.35\varkappa_c$, (c) $\varkappa = 0.27\varkappa_c$, (d) $\varkappa = 0.22\varkappa_c$ and (e) $\varkappa = 0.18\varkappa_c$. The numbers of harmonics including the fundamental fall within the unstable interval $(0, \varkappa_c)$ are (a) $n = 1$, (b) $n = 2$, (c) $n = 3$, (d) $n = 4$ and (e) $n = 5$.

The solutions to the NLS (26) under the same condition as for the case of Fig. 2 are shown in Fig. 3. In both Fig. 2 and Fig. 3 the initial stages of growth of the fundamental mode are consistent with the linear result. While the solutions to the NLS are highly regular, each solution to the MNLS except for the case of Fig. 2 (a) becoms irregular to some degree after an initial interval. This fact can be clearly seen in the corresponding Fourier modes shown in Figs.

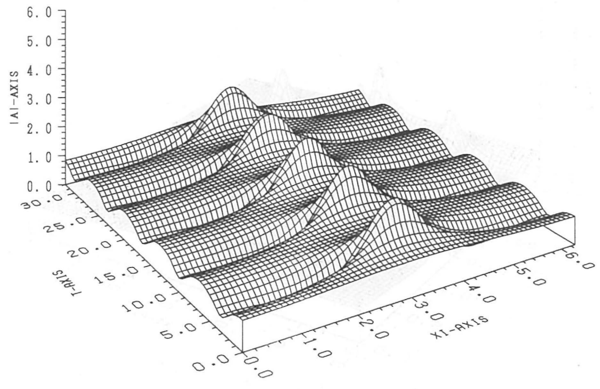
6.0
5.0
4.0
3.0
2.0
1.0
0.0
|A|-AXIS
30.0
25.0
20.0
15.0
10.0
5.0
0.0
T-AXIS
0.0
1.0
2.0
3.0
4.0
5.0
6.0
X1-AXIS

(a)

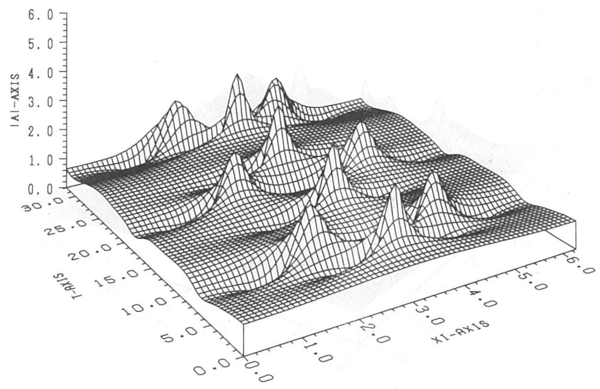
6.0
5.0
4.0
3.0
2.0
1.0
0.0
|A|-AXIS
30.0
25.0
20.0
15.0
10.0
5.0
0.0
T-AXIS
0.0
1.0
2.0
3.0
4.0
5.0
6.0
X1-AXIS

(b)

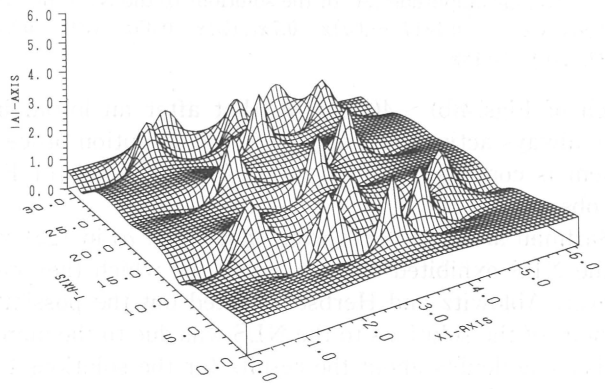
6.0
5.0
4.0
3.0
2.0
1.0
0.0
|A|-AXIS
30.0
25.0
20.0
15.0
10.0
5.0
0.0
T-AXIS
0.0
1.0
2.0
3.0
4.0
5.0
6.0
X1-AXIS

(c)

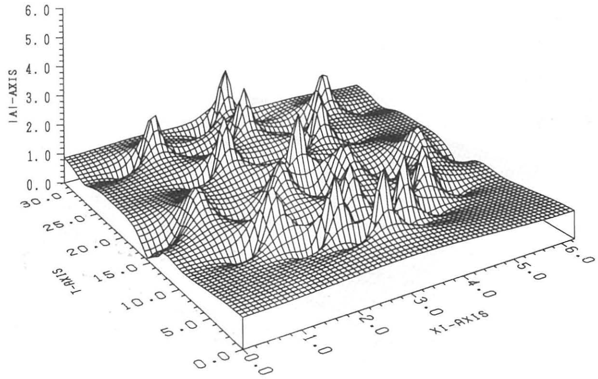

(d)

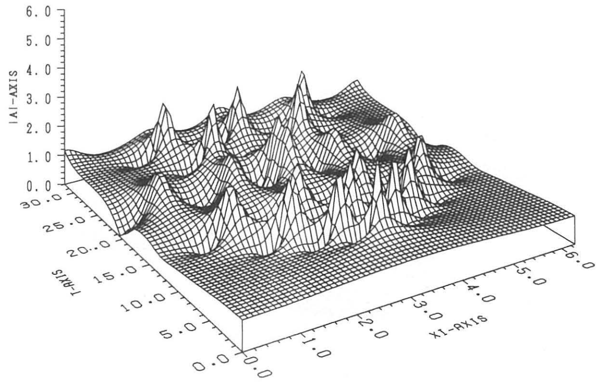

(e)

Fig. 3 The envelope amplitude $|A|$ of the solutions to the NLS for $A(X, 0)=1-0.1\cos(\varkappa X)$. $\beta=0.1817$ $\cdots$.(a)$\varkappa=0.7\varkappa_c$, (b)$\varkappa=0.35\varkappa_c$, (c)$\varkappa=0.27\varkappa_c$, (d)$\varkappa=0.22\varkappa_c$, (e)$\varkappa=0.18\varkappa_c$.

4 and 5. Each of Figs. 4(b) $\sim$ 4(e) shows that after an initial interval many Fourier modes always actively participate in the evolution process, though the number of them is confined. On the other hand, in each of Figs. 5(a) $\sim$5(e) recurrence is observed.

Caponi, Saffman and Yuen[5] reported that when a_0 in (25) was large, the solutions of the NLS exhibited chaotic behaviour which they called confined chaos. However, Ablowitz and Herbst[6] pointed out the possibility that such chaotic behaviour of the solutions to the NLS was due to the numerical scheme used. There is some doubts about the results for the solutions to the NLS by Caponi, Saffman and Yuen[5].

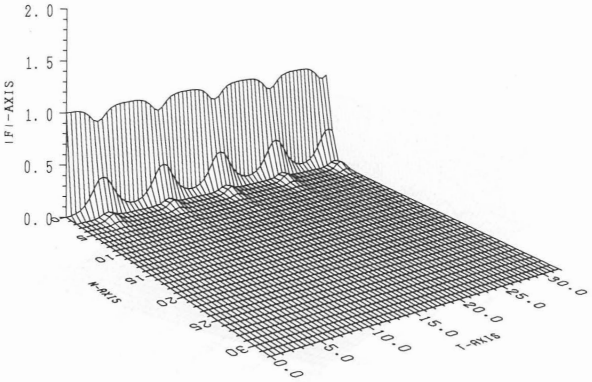
2. 0
1. 5
1. 0
0. 5
0. 0
|F|-AXIS
N-AXIS
T-AXIS
0.0
5.0
10.0
15.0
20.0
25.0
30.0

(a)

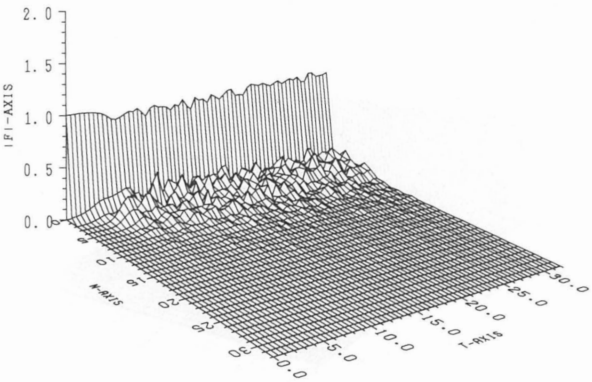
2. 0
1. 5
1. 0
0. 5
0. 0
|F|-AXIS
N-AXIS
T-AXIS
0.0
5.0
10.0
15.0
20.0
25.0
30.0

(b)

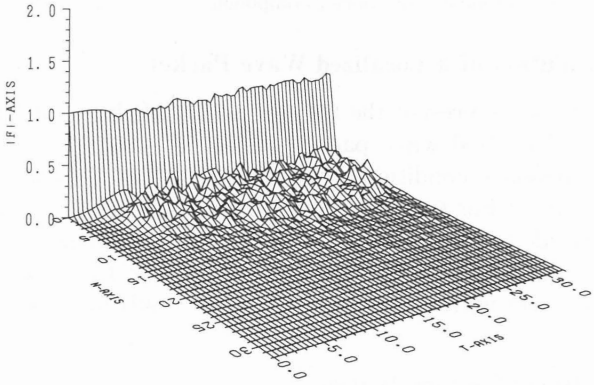
2. 0
1. 5
1. 0
0. 5
0. 0
|F|-AXIS
N-AXIS
T-AXIS
0.0
5.0
10.0
15.0
20.0
25.0
30.0

(c)

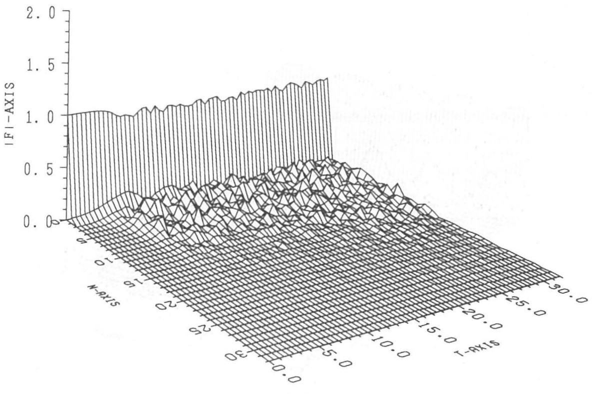

(d)

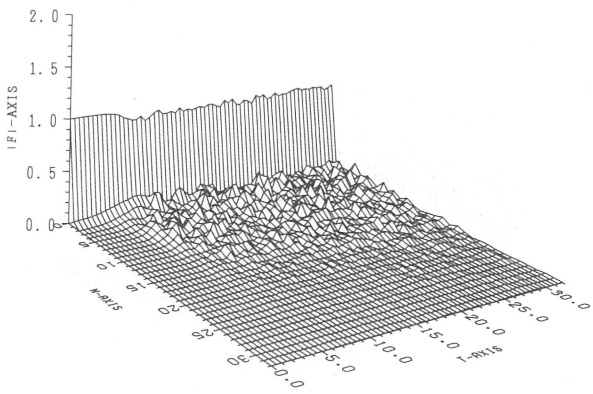

(e)

Fig. 4 The magnitude of the Fourier components of $|A|$ shown in Fig. 2 (MNLS).

5. Time Evolution of a Localized Wave Packet

In this section, we present the time evolution of the solution to the MNLS starting from a localized wave packet $A(X, 0) = \text{sech}\ 3(X-10),\ 0 \leq X \leq 20$. The periodic boundary condition was used for numerical computations. The results are shown in Fig. 6. The initial condition is given in Fig. 6(a) and the envelope amplitude $|A|$ and the wavenumber at $T = 0.8$ are shown in Fig. 6(b) for $k = 0.9$, Fig. 6(c) for $k = 1.0$ and Fig. 6(d) for $k = 1.1$. The small ripples in the left of the main wave in each of Fig. 6(b) $\sim$ 6(d) are due to the periodic boundary condition.

6. Double-Hump Solitary Waves

Here we mention the double-hump solitary wave solutions to the MNLS

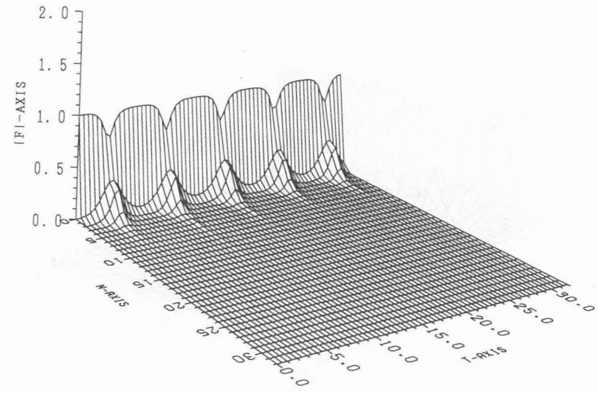
2. 0
1. 5
1. 0
0. 5
0. 0
|F|-AXIS
N-AXIS
T-AXIS
0.0
5.0
10.0
15.0
20.0
25.0
30.0

(a)

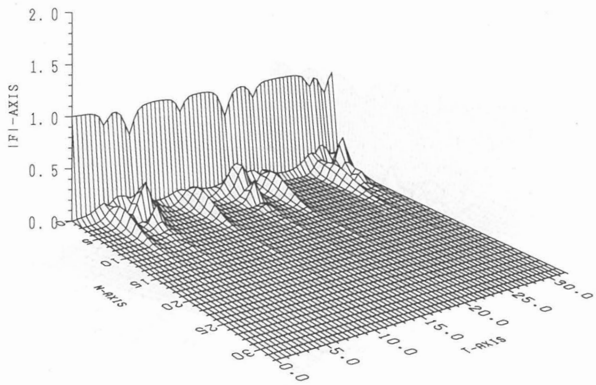
2. 0
1. 5
1. 0
0. 5
0. 0
|F|-AXIS
N-AXIS
T-AXIS
0.0
5.0
10.0
15.0
20.0
25.0
30.0

(b)

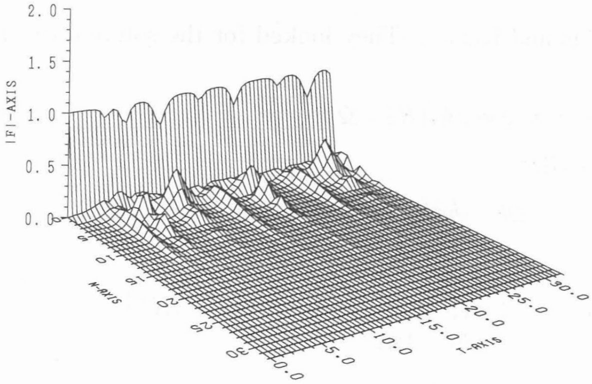
2. 0
1. 5
1. 0
0. 5
0. 0
|F|-AXIS
N-AXIS
T-AXIS
0.0
5.0
10.0
15.0
20.0
25.0
30.0

(c)

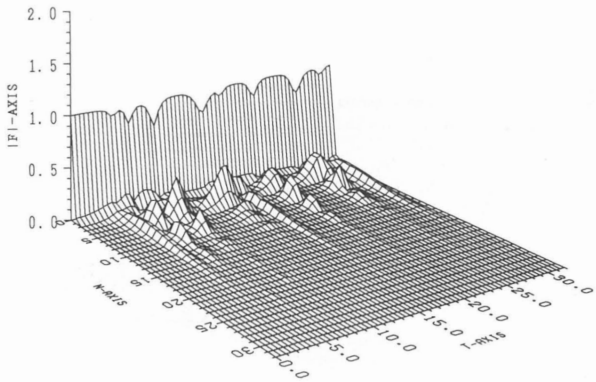

(d)

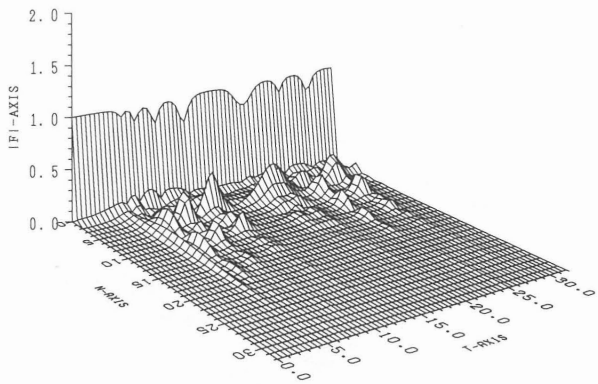

(e)

Fig. 5 The magnitude of the Fourier components of $|A|$ shown in Fig. 3 (NLS).

found by Akylas and Kung[2]. They looked for the solution to the MNLS (19) in the form

$$A = \tilde{b}(\xi)\exp[i(K\xi - \Omega T)], \quad \xi = X - VT. \tag{27}$$

Then, $\tilde{b}(\xi)$ satisfies

$$\bar{\beta}\tilde{b}_{\xi\xi} - \bar{\Omega}\tilde{b} + |\tilde{b}|^2\tilde{b} + i\bar{V}\tilde{b}_\xi + i\gamma\tilde{b}_{\xi\xi\xi} = 0, \tag{28}$$

where

$$\left.\begin{aligned} &\bar{\beta} \equiv \beta - 3\gamma K, \quad \bar{\Omega} \equiv \Omega + KV + \beta K^2 - \gamma K^3, \\ &\bar{V} \equiv V + 2\beta K - 3\gamma K^2. \end{aligned}\right\} \tag{29}$$

Making a scale transformation

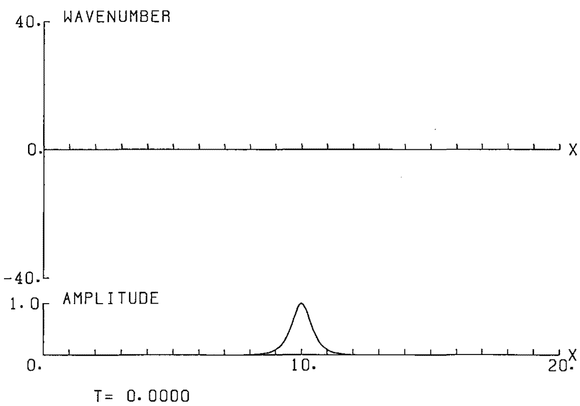

(a)

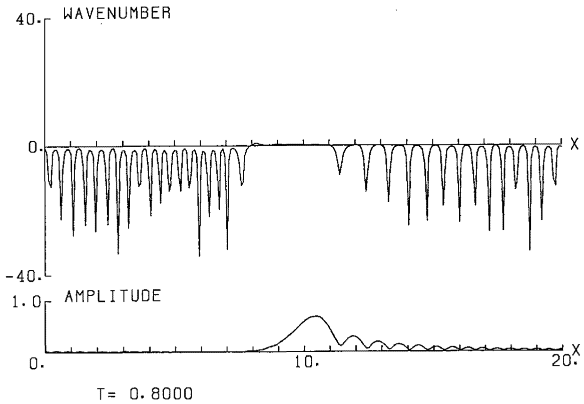

(b)

$$\tilde{b} = |\bar{\Omega}|^{1/2} b, \quad \xi = \left(\frac{\gamma}{|\bar{\Omega}|}\right)^{1/3} \zeta, \tag{30}$$

we have

$$\lambda b_{\zeta\zeta} - sb + |b|^2 b + ivb_\zeta + ib_{\zeta\zeta\zeta} = 0, \tag{31}$$

where

$$\lambda = \frac{\bar{\beta}}{\gamma^{2/3}|\bar{\Omega}|^{1/3}}, \quad v = \frac{\bar{V}}{|\bar{\Omega}|^{2/3}\gamma^{1/3}}, \quad s = \mathrm{sgn}\bar{\Omega}. \tag{32}$$

Writing

$$b = f + ig \quad (f,\ g : \text{real}),$$

we obtain from eq.(31)

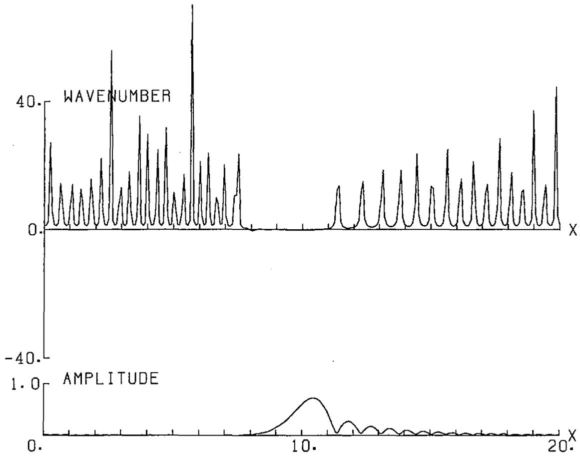

(c)

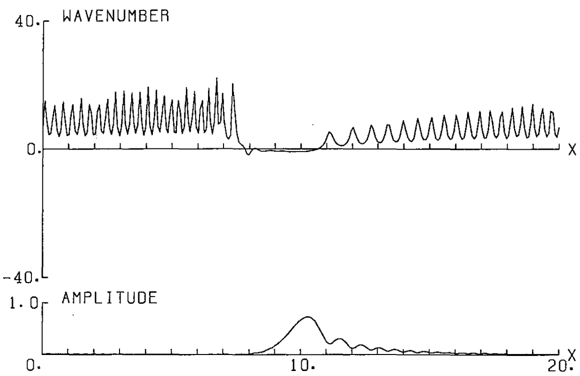

(d)

Fig. 6 Time evolution of a localized wave packet. $\varepsilon=0.05$. (a) $T=0$, (b) $k=0.9$, $T=0.8$, (c) $k=1.0$, $T=0.8$, (d) $k=1.1$, $T=0.8$.

$$\left.\begin{aligned}\lambda f_{\zeta\zeta}-sf+(f^2+g^2)f-vg_\zeta-g_{\zeta\zeta\zeta}&=0,\\ \lambda g_{\zeta\zeta}-sg+(f^2+g^2)g+vf_\zeta+f_{\zeta\zeta\zeta}&=0.\end{aligned}\right\} \tag{33}$$

For a solitary envelope, asymptotic analyses[2] at $\zeta\to\pm\infty$ give rise to the asymptotic behaviour

$$f\sim C_1^{\pm}\exp(\mp(s/\lambda)^{1/2}\zeta),\quad g\sim C_2^{\pm}\exp(\mp(s/\lambda)^{1/2}\zeta)\quad \text{as}\quad \zeta\to\pm\infty, \tag{34}$$

where $C_1^{\pm}$, $C_2^{\pm}$ are constants and

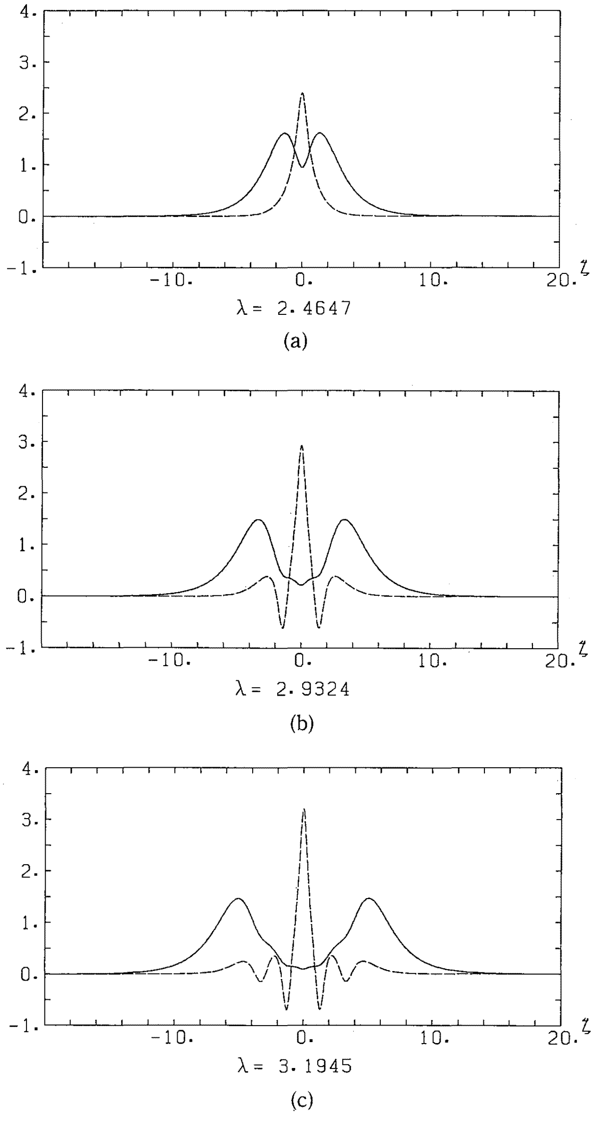

(a)

(b)

(c)

$$v = -\frac{s}{\lambda}, \quad s\lambda > 0. \tag{35}$$

Assuming that f and g are even and odd functions of ζ, respectively, we must impose the conditions

$$f_\zeta = 0, \quad g = 0, \quad g_{\zeta\zeta} = 0 \quad \text{at} \quad \zeta = 0, \tag{36}$$

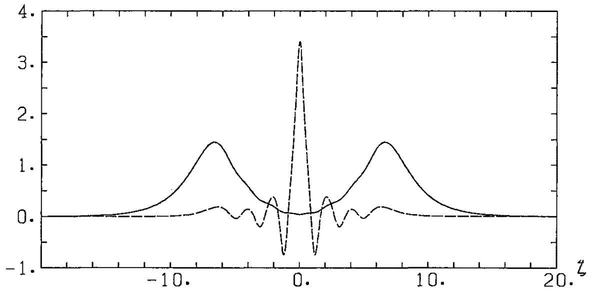

λ= 3.4039

(d)

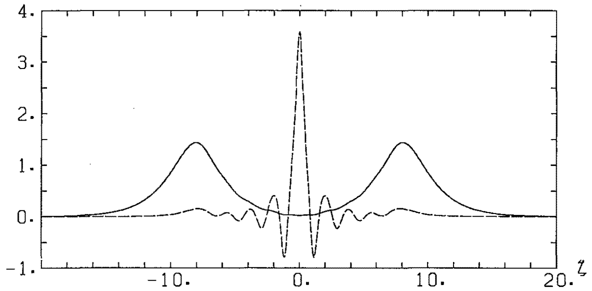

λ= 3.5841

(e)

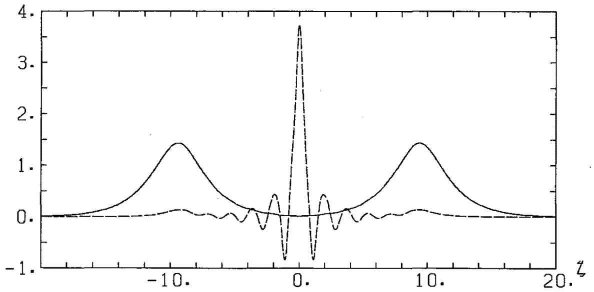

λ= 3.7435

(f)

Fig. 7 Double-hump solitary wave solutions to the MNLS. ——: envelope amplitude, ……: envelope wavenumber. (a)$\lambda=2.4647$, (b)$\lambda=2.9324$, (c)$\lambda=3.1945$, (d)$\lambda=3.4039$, (e)$\lambda=3.5841$, (f)$\lambda=3.7435$.

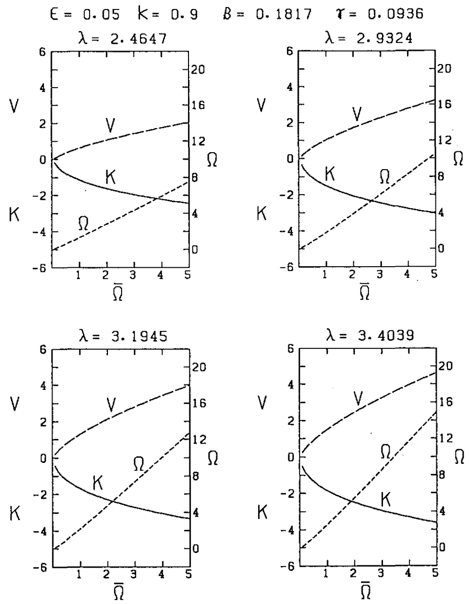

(a)

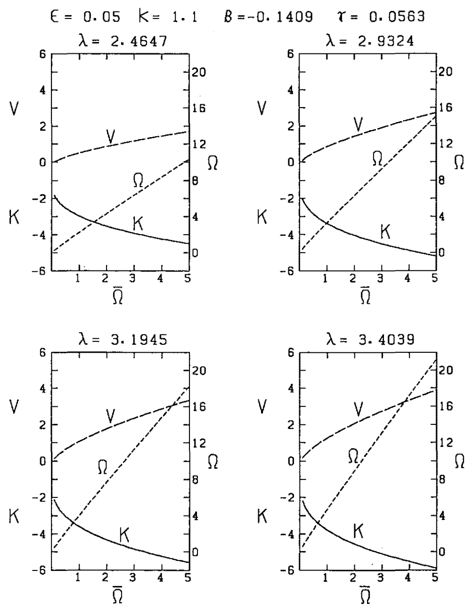

(b)

Fig. 8 *K, V* and Ω as functions of $\bar{\Omega}$. (a)$\varepsilon=0.05$, $k=0.9$, (b)$\varepsilon=0.05$, $k=1.1$.

which provide equations for the unknowns C_1^+, C_2^+ and λ. Thus, only for special values of λ solitary wave solutions of the assumed form can exist. Akylas and Kung[2] gave the first three values of λ and the corresponding solitary waves. We have calculated the next three values of λ and the solitary waves in addition to the first three. Those values (eigenvalues) of λ are $\lambda_1 = 2.4647$, $\lambda_2 = 2.9324$, $\lambda_3 = 3.1945$, $\lambda_4 = 3.4039$, $\lambda_5 = 3.5841$ and $\lambda_6 = 3.7435$. The corresponding solitary waves are shown in Fig. 7. The solid lines denote the envelope amplitude and the broken lines the envelope wavenumber. From eqs.(27) and (30), we can write

$$A = |\bar{\Omega}|^{1/2} b\left(\left(\frac{\bar{\Omega}}{\gamma}\right)^{1/3}\xi\right)\exp[i(K\xi - \Omega T)], \quad \xi = X - VT, \tag{37}$$

where $b(\zeta)$ is the solution corresponding to one of the eigenvalues of λ. Thus, $|\bar{\Omega}|$ is a parameter related to the maximum amplitude and the width of the solitary envelope. For each eigenvalue of λ, if $|\bar{\Omega}|$ is given, K, V, and Ω are determined from eqs.(29), (32) and (35). Consequently, for each eigenvalue of λ, eq.(37) is the one-parameter family of the double-hump solitary waves. In Fig. 8, K, V and Ω are plotted as functions of $\bar{\Omega}$ for the first four eigenvalues of λ. Figure 8(a) shows the case $\varepsilon = 0.05$, $k = 0.9$ and Fig. 8(b) the case $\varepsilon = 0.05$, $k = 1.1$. The solitary wave solutions vanishing at $X \to \pm\infty$ can exist for the case $k = 1.1$, in which the uniform wave solution of the MNLS is modulationally stable.

Acknowledgement

The author would like to thank Dr. M. Okamura for useful discussions. The numerical calculations were made by mean of the FACOM VP-200 of the Computer Center of Kyushu University and the FACOM M-760/8 of the Research Institute for Applied Mechanics, Kyushu University. This work was supported by the Grant-in-Aid for Scientific Research from the Ministry of Education, Science and Culture.

References

1) Kawahara, T.: *Nonlinear self-modulation of capillary-gravity waves on liquid layer,* J. Phys. Soc. Japan **38** (1975) 265.

2) Akylas, T. R. and Kung, T.-J.: *On nonlinear wave envelopes of permanent form near a caustic,* J. Fluid Mech. **214** (1990) 489.

3) Yuen, H. C. and Ferguson, Jr., W. E.: *Relationship between Benjamin-Feir instability and recurrence in the nonlinear Schrödinger equation,* Phys. Fluids **21** (1978) 1275.

4) Fornberg, B. and Whitham, G. B.: *A numerical and theoretical study of certain nonlinear wave phenomena,* Phil. Trans. Roy. Soc. Lond. **A289** (1978) 373.

5) Caponi, A., Saffman, P. G. and Yuen, H. C.: *Instability and confined chaos in a nonlinear dispersive system,* Phys. Fluids **25** (1982) 2159.

6) Ablowitz, M. J. and Herbst, B. M.: *On homoclinic structure and nimerically induced chaos for the nonlinear Schrödinger equation,* SIAM J. Appl. Math. **50** (1990) 339.

(Received 9 July, 1991)